Supporting Information

Arima et al. 10.1073/pnas.1106015108

SI Materials and Methods

DNA and Cell Samples. Genomic DNA was isolated from peripheral blood white cells using a conventional phenol-chloroform method combined with dialysis purification. B cells obtained from peripheral blood were transformed using Epstein-Barr virus.

SNP Genotyping. DNA samples were analyzed using the GeneChip Human Mapping 500K array set (Nsp and Sty arrays) according to the manufacturer's protocol (Affymetrix). Raw array intensity data (CEL files) of 8 of our samples and International HapMap Project phase II Japanese (JPT) samples ($n = 45$) were genotyped simultaneously using BRLMM genotyping software.

SNP Microarray-Based Homozygosity Mapping. To detect the genome-wide structure of ROHs, SNP genotype files (CHP files) were analyzed using the "unpaired LOH detection" function in the Partek Genomics Suite (GS). To obtain maximum resolution for ROH detection, no SNP heterozygosity baseline files were used. We adopted the following thresholds for ROH: 1.0 Mb for first-cousin marriage offspring (patients 2 and 4), 750 kb for other consanguineous marriage offspring (patients 1 and 3), and 500 kb for nonconsanguineous marriage offspring (patient 5). No filtration was used for the unaffected siblings of patient 4. The genome-wide ROH overlap pattern was detected using in-house Ruby script (1) (available on request) and visualized using Partek GS. A region showing ROHs for all of the patients, but not the unaffected siblings, was considered to be a candidate region.

Mutation Search and Sequencing. All PCR reactions used genomic DNA with KOD FX (Toyobo) or ExTaq DNA polymerase HS (Takara) at the appropriate annealing temperature. PCR products were purified for direct sequencing using Exonuclease I (Epicentre) and shrimp alkaline phosphatase (GE Healthcare). Sequencing reactions used a BigDye Terminator v3.1 Cycle Sequencing kit (Applied Biosystems) and electrophoresed using Autosequencer Model 3130xl.

Structural Modeling. Structural models of mutated and nonmutated immunoproteasomes were constructed by exchanging the residues from the constitutive subunits (2) with those from the inducible subunits. Several of the generated models that had minimum energies were further subjected to an experimental data-free energy minimization process using a Crystallography and NMR system (3).

Cell Culture. LCLs and skin fibroblasts were cultured in RPMI 1640 and DMEM, respectively, supplemented with 10% FBS, 100 IU/mL penicillin G, and 100 mg/mL streptomycin.

Protein Extracts, Immunological Analysis, and Antibodies. Cells were lysed in ice-cold lysis buffer [50 mM Tris-HCl (pH 7.5), 0.5% (vol/vol) Nonidet P-40, and 1 mM DTT with 2 mM ATP and 5 mM $MgCl_2$]. The extracts were clarified by centrifugation at 20,000 × *g* for 10 min at 4 °C. The supernatants were subjected to SDS/PAGE (12.5% for proteasome subunits or 7.5% for polyubiquitinated proteins) or analyzed by glycerol gradient centrifugation. The separated proteins were transferred onto a polyvinylidene difluoride membrane and incubated with the indicated antibodies. Membranes were developed using the ECL Plus Western Blotting Detection system (GE Healthcare).

Antibodies against proteasome β1, β2, β5, β7, β1i, β2i, and β5i subunits and hUmp-1 were raised in rabbits using recombinant proteins (4). An anti-β4 subunit monoclonal antibody (mAb), anti-Rpt6 mAb, and anti-α6 subunit mAb (MCP20) were purchased from ENZO. An antiubiquitin antibody (Dako), anti–K48- and anti–K63-linked ubiquitin antibodies (Millipore) (4), horseradish peroxidase (HRP)-conjugated antimouse, and antirabbit IgG antibodies (Jackson ImmunoResearch Laboratories) were used for Western blot analysis.

Glycerol Density Gradient Separation. Proteins from cell extracts (600 μg) were separated into 32 fractions by centrifugation (22 h at 100,000 × *g*) in 8–32% (vol/vol) linear gradients as described previously (6).

Assays for Proteasome Peptidase Activities. Chymotrypsin-like, trypsin-like, and caspase-like activities were determined using the fluorescent peptide substrates succinyl-Leu-Leu-Val-Tyr-7-amido-4-methylcoumarin (Suc-LLVY-MCA), butyloxycarbonyl-Leu-Arg-Arg-4-metylcoumarin (Boc-LRR-MCA), and benzyloxycarbonyl-Leu-Leu-Glu-methylcoumarylamine (Z-LLE-MCA), as described previously (7). The assays for chymotrypsin-like and caspase-like activities were carried out in the presence of 0.03% SDS, which is a potent artificial activator of the latent 20S proteasome.

Assays for Proteolytic Degradation in Vitro. Degradation of the recombinant 35S-labeled ornithine decarboxylase (ODC) was assayed in the presence of ATP, at 20 min and 40 min, as described previously (8). Data were shown in ^{35}S-ODC degradation (%).

Oxidized Protein Detection. Oxidized proteins were visualized using an OxyBlot protein oxidization detection kit (Millipore) following the supplier's protocol.

Immunohistochemistry. Immunohistochemistry used a standard indirect immunofluorescence method. Sections of formalin-fixed, paraffin-embedded tissues were deparaffinized and microwave epitope retrieval was performed after pretreatment at 80 °C for 30 min in 10 mM citrate buffer (pH 6.0). Endogenous peroxidase was inactivated with a 3% H_2O_2 solution following epitope retrieval. After blocking in 5% normal horse serum in PBS, the slides were incubated for 60 min at room temperature with rabbit polyclonal antiubiquitin antibodies (Dako) or a mouse monoclonal antihuman CD68 antibody (ProSci).

Sections were then incubated with FITC-conjugated donkey antimouse IgG or tetramethylrhodamine isothiocyanate-conjugated donkey antirabbit IgG (Jackson ImmunoResearch) in 5% normal horse serum in PBS for 30–45 min at room temperature. After washing in PBS, the slides were mounted in Vectashield mounting medium (Vector Laboratories) and scanned by confocal microscopy (LSM5, PASCAL; Carl Zeiss). Control experiments were performed to ensure the isotype specificity for each of the secondary antibodies. Negative control studies used species-specific IgG as primary antibodies.

Electrophoretic Mobility Shift Assay (EMSA) Using NF-κB Consensus Oligonucleotides. Nuclear proteins were extracted using a Nuclear Extract kit (Active Motif). Nuclear extracts (4 μg) were used for the EMSA assay using an EMSA kit (Pierce). The consensus oligonucleotide sequences for the NF-κB binding motif were: 5′-AGT TGA GGG GAC TTT CCC AGG C-3′ (sense) and 5′-GCCTGGGAAAGTCCCCTCAACT-3′ (antisense). For the competition assay, a nuclear extract was preincubated with an unlabeled oligonucleotide followed by addition of a [γ-^{32}P]-ATP labeled NF-κB probe. Samples were loaded onto 4% polyacrylamide gels (38:1) in 0.5 × TBE and run at 1 W at room

temperature. Gels were dried and exposed to a Storage Phosphor Screen BAS-IP (GE Healthcare). To confirm the integrity of NF-κB binding, anti-p65 and anti-p50 (Santa Cruz Biotechnology) antibodies were used for the supershift assay.

1. Kurotaki N, et al. (2011) Identification of novel schizophrenia Loci by homozygosity mapping using microarray analysis. *PLoS ONE* 6:e20589.
2. Unno M, et al. (2002) The structure of the mammalian 20S proteasome at 2.75 A resolution. *Structure* 10:609–618.
3. Brünger AT, et al. (1998) Crystallography & NMR system: A new software suite for macromolecular structure determination. *Acta Crystallogr D Biol Crystallogr* 54: 905–921.
4. Hirano Y, et al. (2008) Dissecting beta-ring assembly pathway of the mammalian 20S proteasome. *EMBO J* 27:2204–2213.
5. Newton K, et al. (2008) Ubiquitin chain editing revealed by polyubiquitin linkage-specific antibodies. *Cell* 134:668–678.
6. Hirano Y, Murata S, Tanaka K (2005) Large- and small-scale purification of mammalian 26S proteasomes. *Methods Enzymol* 399:227–240.
7. Murata S, et al. (2007) Regulation of CD8+ T cell development by thymus-specific proteasomes. *Science* 316:1349–1353.
8. Hirano Y, et al. (2005) A heterodimeric complex that promotes the assembly of mammalian 20S proteasomes. *Nature* 437:1381–1385.
9. Feng DF, Doolittle RF (1987) Progressive sequence alignment as a prerequisite to correct phylogenetic trees. *J Mol Evol* 25:351–360.

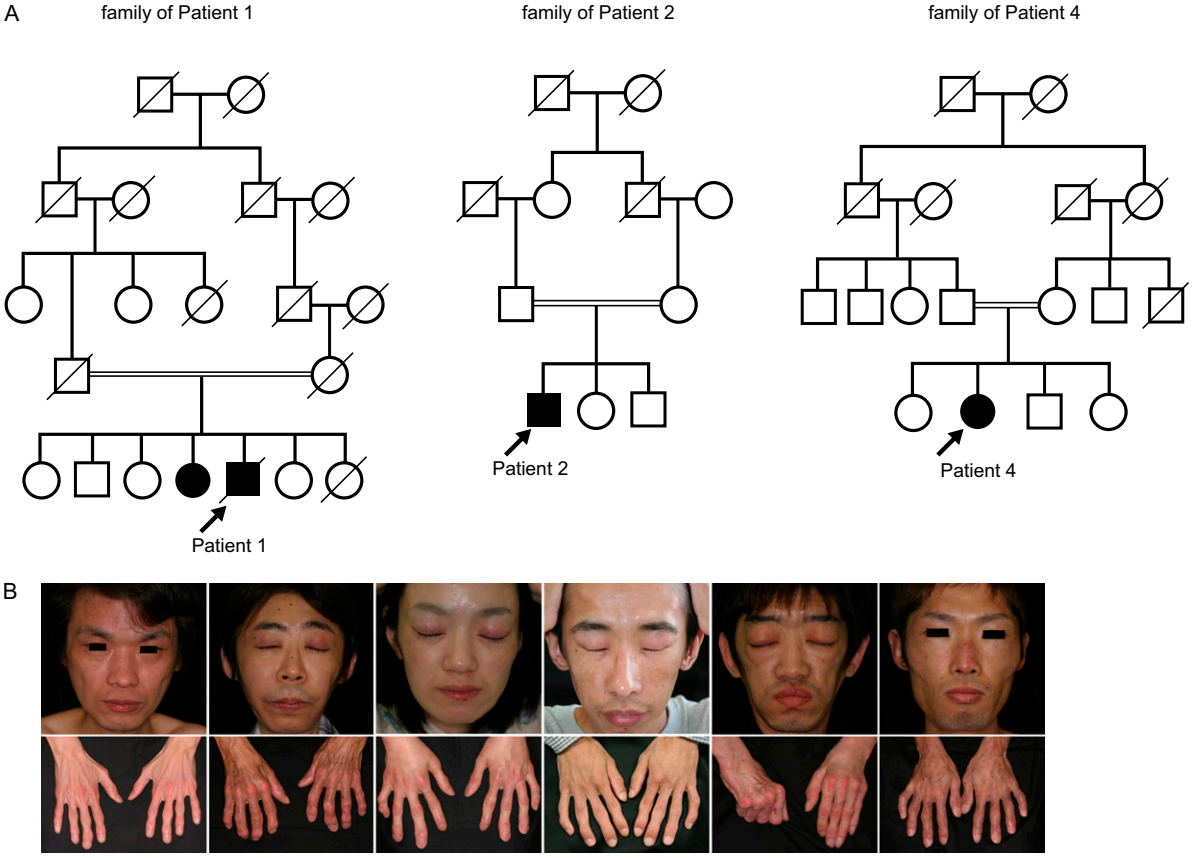

Fig. S1. (Continued)

C

	Patient 1	Patient 2	Patient 3	Patient 4	Patient 5	Patient 6	Patient 7	patient's father	Control 1	Control 2	Control 3	Control 4	Control 5	Control 6	Control 7
rs2857103	TT	TT	TT	TT	TT	TT	TT	TT	TT	GG	GT	GG	GG	GT	TT
rs10484565	GG	GG	GG	GG	GG	GG	GG	GG	AG	AG	GG	GG	GG	GG	GG
rs4148876	GG	GG	GG	GG	GG	GG	GG	GG	GA	AA	GA	AA	AA	GG	GG
rs241439	AA	AA	AA	AA	AA	AA	AA	AA	AA	AA	AA	AC	AC	AC	AA
rs241439	CC	CC	CC	CC	CC	CC	CC	CC	AC	AC	AC	AC	AA	AC	CC
rs241433	GG	GG	GG	GG	GG	GG	GG	GA	GA	GG	AA	GG	GA	GG	GA
rs241433	TT	TT	TT	TT	TT	TT	TT	TT	TT	GT	TT	GG	GT	GT	TT
rs4148872	GG	GG	GG	GG	GG	GG	GG	GG	GG	GG	GG	GG	GG	GA	GG
rs241429	CC	CC	CC	CC	CC	CC	CC	CC	CC	TC	CC	TT	TC	TC	CC
rs3819717	TT	TT	TT	TT	TT	TT	TT	TC	TC	TC	CC	TT	TC	TT	TC
rs241425	TT	TT	TT	TT	TT	TT	TT	TC	TC	CC	TT	CC	TC	TC	TT
rs4148870	AA	AA	AA	AA	AA	AA	AA	AA	GA	GA	GA	AA	GA	GA	GG
rs4713598	TT	TT	TT	TT	TT	TT	TT	TG	TG	TG	TT	GG	TG	TG	TT
rs3763366	CC	CC	CC	CC	CC	CC	CC	CC	CG	CG	GG	CC	CG	CG	GG
rs3763364	TT	TT	TT	TT	TT	TT	TT	TA	TT	TT	TT	AA	TT	TT	TT
rs3763349	CC	CC	CC	CC	CC	CC	CC	CC	TC	TC	TT	CC	TC	TC	TT
PSMB8 exon 5	TT	TT	TT	TT	TT	TT	TT	TG	GG	GG	GG	GG	GG	GG	GG
rs9357155	GG	GG	GG	GG	GG	GG	GG	GA	GA	GG	GG	GG	GG	GG	GG
rs9276810	GG	GG	GG	GG	GG	GG	GG	GA	GA	GG	GG	AA	GA	GA	GG
rs6924102	AA	AA	AA	AA	AA	AA	AA	AG	AG	AG	AA	GG	AG	AG	AA
rs4713599	CC	CC	CC	CC	CC	CC	CC	CA	AA	AA	AA	AA	AA	AA	AA
rs2071543	CC	CC	CC	CC	CC	CC	CC	CA	CA	CC	CC	CC	CC	CC	CC
rs2071463	GG	GG	GG	GG	GG	GG	GG	GG	AG	GG	AA	GG	AG	GG	AG
rs2071541	CC	CC	CC	CC	CC	CC	CC	CT	TT	CT	TT	TT	TT	TT	TT
rs2071540	GG	GG	GG	GG	GG	GG	GG	GG	AG	GG	AA	GG	AG	AG	AA
rs1057373	TT	TT	TT	TT	TT	TT	TT	TG	GG	TG	GG	GG	GG	GG	GG
rs4711312	GG	GG	GG	GG	GG	GG	GG	GA	AA	GA	AA	AA	AA	AA	AA
rs735883	CC	CC	CC	CC	CC	CC	CC	CT	CT	CT	CC	TT	CT	CT	CC
rs2071482	TT	TT	TT	TT	TT	TT	TT	TG	GG	TG	GG	GG	GG	GG	GG
rs4148882	TT	TT	TT	TT	TT	TT	TT	TT	TC	TT	CC	TT	TC	TC	CC
rs12527715	CC	CC	CC	CC	CC	CC	CC	CT	TT	CT	TT	TT	TT	TT	TT
rs12529313	GG	GG	GG	GG	GG	GG	GG	GA	AA	GA	AA	AA	AA	AA	AA
rs2395269	GG	GG	GG	GG	GG	GG	GG	GT	TT	GT	TT	TT	TT		
rs2071538	CC	CC	CC	CC	CC	CC	CC	CC	CC	CC	TC	CC	TC	TC	TC
rs4148880	GG	GG	GG	GG	GG	GG	GG	GA	AA	GA	AA	AA	AA	AA	AA
rs1351383	GG	GG	GG	GG	GG	GG	GG	GT	TT	GG	TT	GG	GT	GT	TT

Fig. S1. (Continued)

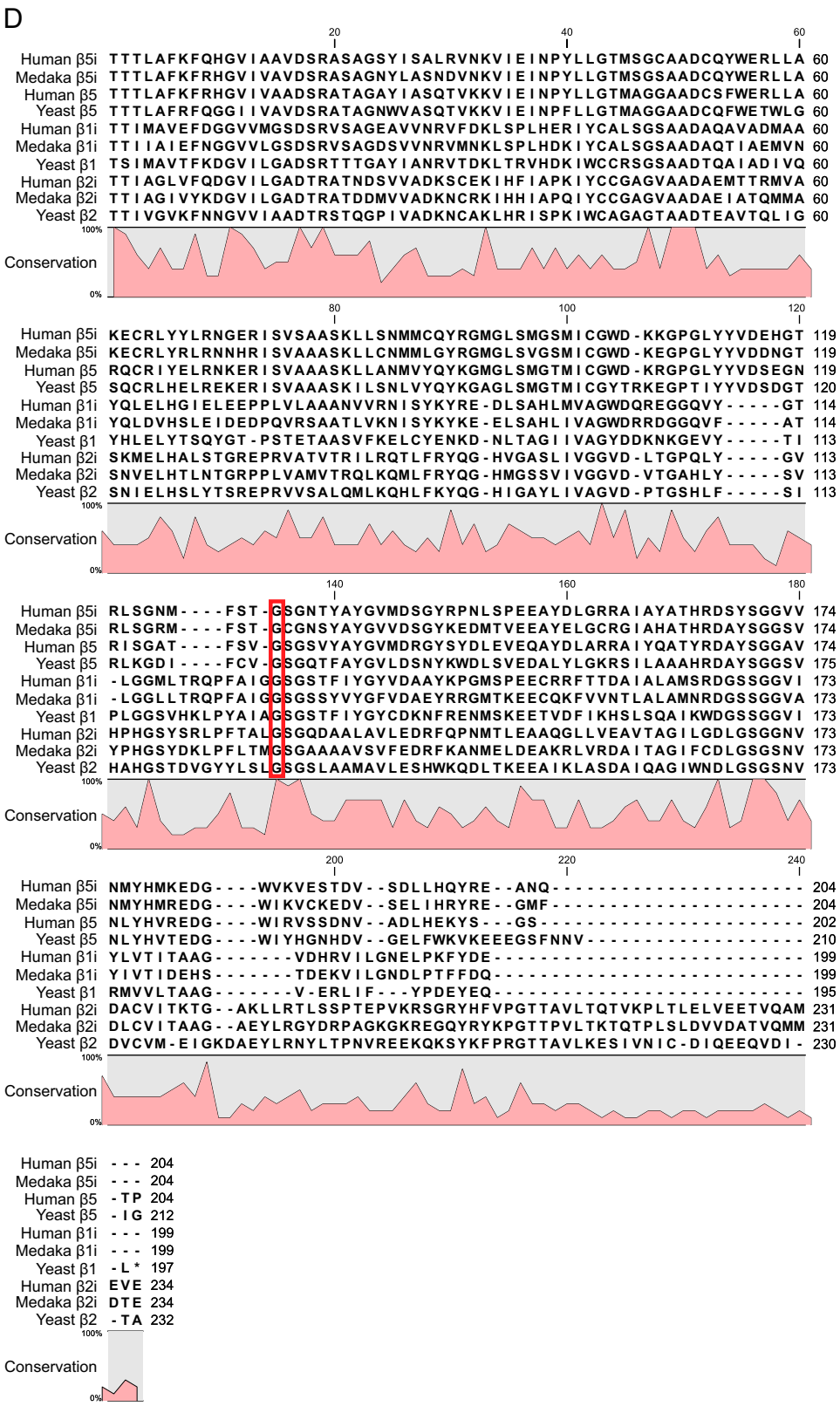

Fig. S1. NNS patients and their consanguineous family histories. (*A*) The families of patients 1, 2, and 4 contain offspring from consanguineous marriages. Solid circles and squares indicate patients with NNS. Arrows, double lines, and diagonal lines indicate probands, consanguineous marriages, and deceased individuals, respectively. (*B*) Photograph of the characteristic thin facial appearance and elongated clubbed fingers in patients 2–7. (*C*) Haplotypes around the *PSMB8* gene mutation. SNPs around *PSMB8* exon 5 were genotyped for seven NNS patients, the father of one patient, and nine controls. All patients shared the same haplotype within this region, which suggests that this mutation was transmitted from a single founder. Control: healthy control in general population. (*D*) Evolutionary conservation of proteasome subunits β5i, β5, β1i, β1, β2i, and β2. Each amino acid sequence is shown in its mature form. The red box indicates the position of the NNS mutation. Multiple amino acid sequence alignment using CLC Sequence Viewer version 6.4, implementing the progressive alignment algorithm (9).

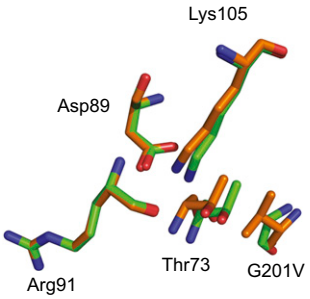

Fig. S2. Computer modeling of mutant β5i. The catalytic residues of proteasome $\beta5i^{G201V}$ and β5i subunits. Thr73 is the most important catalytic residue within the N terminus of mature β5i. Only the amino acid side chains are shown. Nitrogen and oxygen atoms are blue and red, respectively. The G201V structure is shown in orange and the wild type is shown in green.

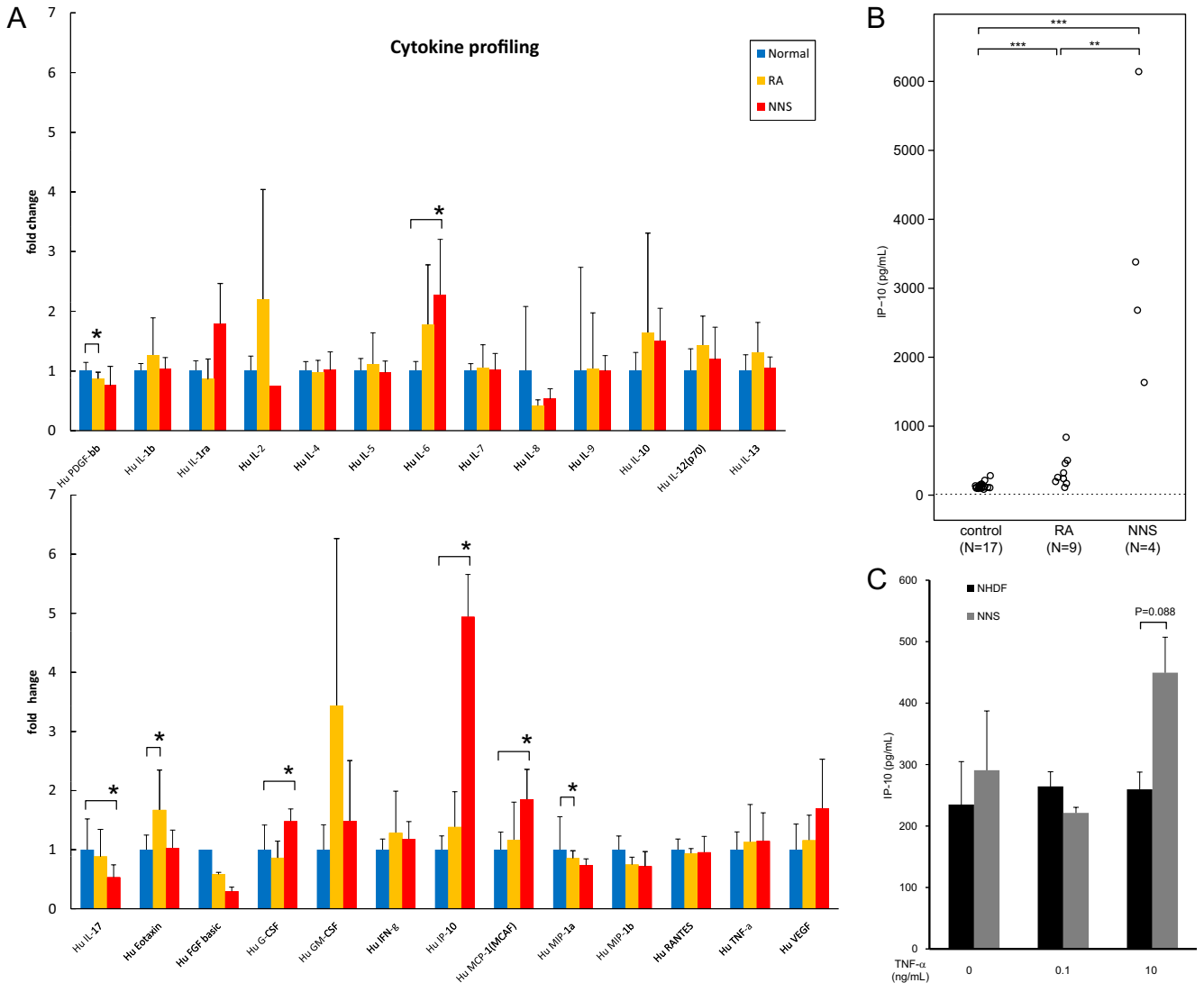

Fig. S3. Cytokine profiles in sera and conditional media from cultured fibroblasts. (*A*) Serum samples were obtained from healthy controls (n = 16), rheumatoid arthritis patients (RA; n = 10), and NNS patients (n = 4). The concentrations of 27 different cytokines were determined using a multiplex bead-based ELISA on a suspension array. Error bars indicate SD of the mean. P values were calculated using two-tailed Welch's t test. *$P \leq 0.05$. (*B*) IP-10 concentration in sera from patients with NNS and RA. IP-10 levels in sera were determined by ELISA on a suspension array. **$P \leq 0.01$, ***$P \leq 0.001$; Mann-Whitney u test. (*C*) IP-10 production by cultured fibroblasts. The concentrations of IP-10 in conditioned media were determined by ELISA (R&D Systems) using triplicate measurements. P, two-tailed Welch's t test.

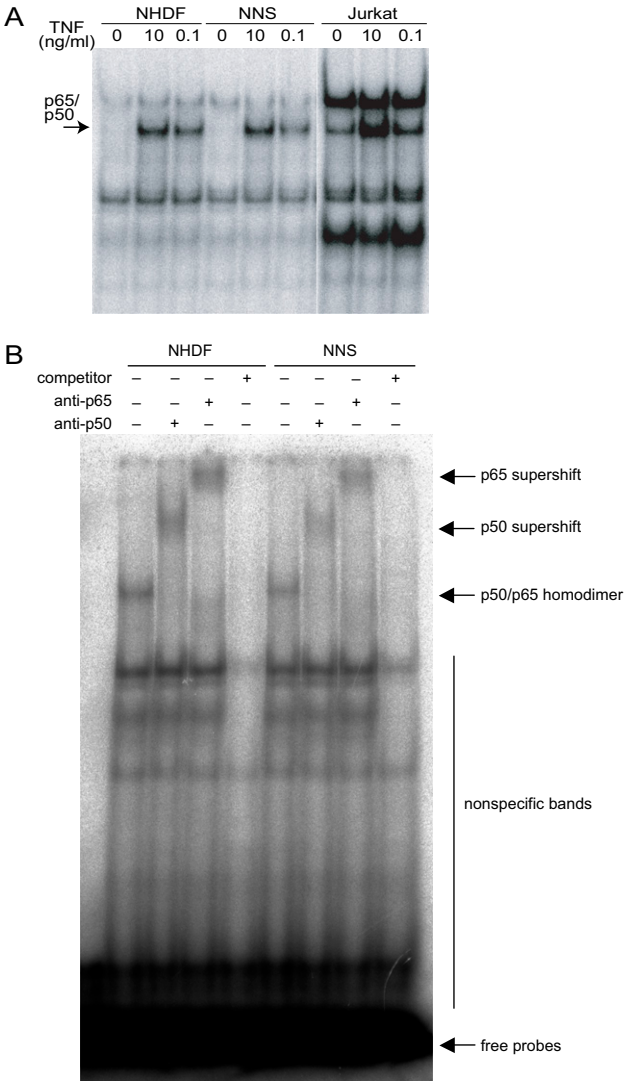

Fig. S4. NF-κB activity in fibroblasts from a NNS patient. (*A*) EMSA for NF-κB. EMSA with an NF-κB consensus probe was performed using nuclear extracts from normal human dermal fibroblast (NHDF), NNS fibroblasts, and Jurkat cells. The NF-κB signal was activated by TNF-α (10 ng/mL or 0.1 ng/mL) in all cell lines. (*B*) EMSA, using a specific antibody, was performed on nuclear extracts from NHDF and NNS after stimulation with TNF-α (10 ng/mL). The signal derived from the p50/p65 heterodimer was confirmed as a supershifted signal in both p50 and p65.

Table S1. Clinical features of our NNS patients compared to JMP syndrome

Patient	1	2	3	4	5	6	7	JMP (3 cases)
Present age, y (at death)	(47)	37	38	31	35	33	32	26–35
Sex	M	M	M	F	M	M	M	M/F
Parental consanguinity	+	+	–	+	–	–	–	–
Family history	+	–	–	–	–	–	–	±
Age at onset of pernio-like rash	–	2 mo	3 mo	6 mo	2 y	1 y	Infancy	–
Heliotrope-like periorbital rash	–	–	+	+	+	+	–	–
Nodular erythema-like eruptions	+	+	+	+	+	+	+	+
Age at onset of fever	12 y	Infancy	7 y	11 mo	2 y	2 y 4 mo	–	–
Partial lipomuscular atrophy	++	+	+	+	+	++	+	+
Long clubbed fingers	+	+	+	+	+	+	+	+
Joint contractures	++	–	+	+	+	++	+	++
Hyperhidrosis	–	+	+	++	–	–	+	NA
Short stature	–	–	–	–	–	+	–	+
Seizures	–	–	–	–	–	–	–	+
Low IQ	+	–	–	–	–	–	–	–
Microcytic anemia	–	+	+	+	+	+	+	+
Elevated ESR/CRP	+	+	+	+	+	+	+	+
High serum CPK	–	+	+	+	–	+	–	+
Hyper-γ-globulinemia	+	+	+	++	+	+	+	+
Antinuclear antibody titer	<40	<40	160	640	80	40	40	–
Positive autoantibody	–	–	MPO-ANCA	dsDNA	SS-A	dsDNA	–	–
Diabetes	+	–	–	–	–	–	–	–
Hypertriglyceridemia	–	–	–	+	+	+	+	–
Low HDL cholesterol	NA	+	–	+	+	+	+	+
Hepatosplenomegaly	+	NA	+	+	+	+	NA	+
Basal ganglia calcification	–	+	+	+	+	+	+	+
Reference	1, 2	3		4				5

All NNS patients have a c.602G > T mutation. M, male; F, female; y, years; mo, months; NA, not assessed; MPO, myeloperoxidase; ANCA, antineutrophil cytoplasmic antibody; ds, double stranded; JMP, joint contracture, muscular atrophy, microcytic anemia, and panniculitis-induced lipodystrophy.

1. Tanaka M, et al. (1993) Hereditary lipo-muscular atrophy with joint contracture, skin eruptions and hyper-gamma-globulinemia: A new syndrome. *Intern Med* 32:42–45.
2. Oyanagi K, et al. (1987) An autopsy case of a syndrome with muscular atrophy, decreased subcutaneous fat, skin eruption and hyper gamma-globulinemia: Peculiar vascular changes and muscle fiber degeneration. *Acta Neuropathol* 73:313–319.
3. Muramatsu T, Sakamoto K (1987) Secondary hypertrophic osteoperiostosis with pernio (Nakajo). *Skin Res* 29:727–731.
4. Kasagi S, et al. (2008) A case of periodic-fever-syndrome-like disorder with lipodystrophy, myositis, and autoimmune abnormalities. *Mod Rheumatol* 18:203–207.
5. Garg A, et al. (2010) An autosomal recessive syndrome of joint contracture, muscular atrophy, microcytic anemia, and panniculitis-associated lipodystrophy. *J Clin Endocrinol Metab* 95: E48–E63.